# Distribution of Carbon Black in Semicrystalline Polypropylene Studied by Transmission Electron Microscopy

**JIYUN FENG, JIANXIONG LI, CHI-MING CHAN**

Department of Chemical Engineering, Advanced Engineering Materials Facility, Hong Kong University of Science and Technology, Clear Water Bay, Kowloon, Hong Kong

*Received 19 April 2001; accepted 20 October 2001*

**ABSTRACT:** Polypropylene (PP) samples filled with different carbon blacks (CB) were prepared by the conventional melt-mixing method. The distribution of the CB in the PP matrix was investigated by using the $RuO_4$ vapor-staining technique and transmission electron microscopy (TEM). Our results indicate that amorphous regions of PP are sandwiched between the crystalline lamellae. The thickness of individual amorphous layers is a few nanometers. The amorphous region was measured to be about 45 wt % using a differential scanning calorimeter (DSC). The thickness of the lamellae is much smaller than the dimensions of the CB particles, and the CB particles or aggregates are dispersed inside the spherulites. There is a thin layer of amorphous PP encapsulating the CB particles and aggregates. © 2002 Wiley Periodicals, Inc. J Appl Polym Sci 85: 358–365, 2002

**Key words:** polypropylene; carbon black; amorphous layer; transmission electron microscopy; semicrystalline polymers

## INTRODUCTION

It is well known that the electrical properties of carbon black (CB)–filled conductive polymers can vary significantly with the distribution of the carbon black in the polymer matrix. For example, the positive temperature coefficient (PTC) and negative temperature coefficient (NTC) effects change with varying the amounts of the CB. Determining the CB distribution in a polymer matrix will lead to a full understanding of the mechanisms of the PTC and NTC effects. However, up to now, only limited information about the dispersion of CB in semicrystalline polymers has been available.[1–7] The electrical properties of CB-filled conductive polymers have been mostly interpreted using schematic models.

With the current development of staining techniques for polymers, most semicrystalline polymers can be stained and their morphologies can be imaged with transmission electron microscopy (TEM).[8–12] For example, Kanig and Kolloid[8] utilized chlorosulfonic acid and uranyl acetate to stain polyethylene (PE) and studied its morphology with TEM. They revealed that PE consists of alternate crystalline and amorphous layers, although PE's crystalline lamellae are not flat and can be twisted. The thickness (about 15 nm) of individual lamellae imaged under TEM is consistent with the long periodicity calculated on the basis of the results of small-angle X-ray diffrac-

*Correspondence to:* C.-M. Chan (kecmchan@ust.hk).

Contract grant sponsor: Industry and Technology Development Council; contract grant number: AF/155/99.

Contract grant sponsor: Hong Kong Government Research Grant Council; contract grant number: HKUST 6123/97P.

Journal of Applied Polymer Science, Vol. 85, 358–365 (2002)

tion. Trent et al.[11] introduced $RuO_4$ to stain various polymers, including saturated and unsaturated crystalline polymers. By using the $RuO_4$ vapor-staining technique and TEM, Li et al.[12,13] investigated the arrangement of lamellae in $\alpha$- and $\beta$-polypropylene (PP) spherulites. Their results indicated that the amorphous layers can absorb more $RuO_4$, such that the amorphous layers and lamellae can be identified under TEM imaging. The architecture of the lamellae in the $\alpha$- and $\beta$-PP spherulites has been clarified. Likewise, using staining techniques, such as $RuO_4$ vapor staining, it is possible to stain CB-filled semicrystalline polymer composites and produce images of the detailed morphology of CB-filled conductive polymer composites using TEM.

In the present work, various types of conductive carbon black were melt-mixed with semicrystalline polypropylene (PP). The resultant conductive PP composites were stained with a $RuO_4$ vapor and their morphologies were examined by TEM. The objective of the investigation was to elucidate the CB distribution in semicrystalline PP.

## EXPERIMENTAL

The polymer used in this study was isotactic PP (Profax PD382, MFI = 3 g/10 min) from Himont (USA). The CBs were N660 from Columbian Chemicals (USA), V-XC72 from Cabot (USA), and Ketjenblack EC-300J from Nobel Azoko (The Netherlands), respectively. The PP resin was compounded with 10 wt % of the different CBs using a Haake mixer at 200°C and 30 rpm for 15 min. The resultant compounds were compressed into 2-mm-thick plates using a hot press at 200°C and 16 MPa. Finally, the compression-molded plates were kept in the mold under pressure and cooled first by compressed air from 200 to 140°C and then by tap water from 140°C to room temperature.

The melting behaviors of the PP and CB-filled PP composites were determined by using a TA 2910 differential scanning calorimeter (DSC; TA Instruments, New Castle, DE). The instrument was calibrated with indium as a standard. All the experiments were conducted at a heating rate of 10°C/min under a continuous $N_2$ purge. The purge rate of $N_2$ was 100 mL/min. The weight of the samples was 10–12 mg. The peak value in the plot of heat flow against temperature was taken as the melting temperature ($T_m$) of the sample and the fusion heat of PP was estimated from the peak area from the first heating scan.

The weight fraction crystallinity $X_c$ of the PP component was determined using the specific heat of fusion, according to the following equation:

$$X_c = \frac{\Delta H_i}{\Delta H_i^\circ} \times 100\% \quad (1)$$

where $\Delta H_i$ is the measured specific heat of fusion of the PP component of the specimens and $\Delta H_i^\circ$ is the standard specific fusion heat of the crystalline phase (178 J/g was used for the $\alpha$-phase of the PP crystals).[14]

To investigate the detailed morphology of the CB distribution in the PP, the PP sample and the CB-filled PP composites were stained using the $RuO_4$ vapor-staining technique.[12,13] Before staining, thin strips with a cross section of 0.3 × 0.2 mm were cut from the compression-molded PP and PP composites. The strips were embedded in an epoxy resin and cured at room temperature for 48 h. The embedded specimens were trimmed first using a razor blade and then using an ultracut microtome equipped with a glass knife. After trimming, the specimens were exposed to the $RuO_4$ vapor in a sealed test tube at room temperature for 48–72 h. After staining, the specimens were washed in a 3% aqueous sodium periodate solution and distilled water, sequentially. Finally, they were dried in a desiccator before microtomy.

The microtomy was performed on a Leica Ultracut R microtome (Leica, Deerfield, IL) at room temperature. A top layer of about 0.5 $\mu$m thickness was first removed from the stained specimens using a glass knife, and the ultrathin sections of about 70 nm in thickness were cut from the internal materials of the stained specimens using a 45° Diatome diamond knife. The cutting velocities for the glass knife and the diamond knife were 5.0 and 1.0 mm/s, respectively. The ultrathin sections were mounted on 200-mesh copper grids and dried in a desiccator for more than 24 h before the TEM examination. The TEM examination of the ultrathin sections was conducted on a JEOL 100CX II electron transmission microscope (JEOL, Peabody, MA) operated at an accelerating voltage of 80 kV.

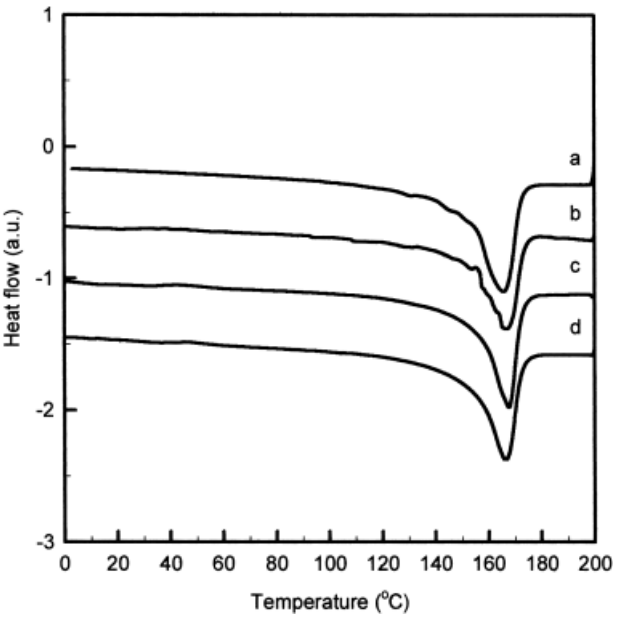


**Figure 1** DSC thermograms of PP and CB-filled PP composites: (a) PP, (b) 10 wt % N660-filled PP, (c) 10 wt % V-XC72–filled PP, and (d) 10 wt % Ketjenblack-filled PP.

## RESULTS AND DISCUSSION

### Lamellar Structure of PP

To study the CB distribution in semicrystalline polymers, PP was used because the staining technique for PP has been fully established.[11–13] Before TEM examination, the crystallinities and melting points of the PP and PP composites filled with different CBs were determined by DSC measurements. Figure 1 shows the DSC thermographs of the PP and CB-filled PP composites. From the melting peak positions, the crystals in the PP and the PP composites were identified as the $\alpha$-phase.[14] In addition, the crystallinities of the PP and PP composites were calculated, the results of which are summarized in Table I. The DSC results indicate that the addition of CB has no significant influence on the crystallinities of PP components and the crystallinity was measured to be around 57 wt %.

Figure 2 shows the TEM micrograph of an ultrathin section of the PP stained with the $RuO_4$ vapor. At high magnification, it can clearly be seen that the thickness of the lamellae is less than 10 nm. The lamellae appear to interweave together, forming small trellises. Additionally, the characteristic cross-hatched structure of $\alpha$-PP, with shorter daughter lamellae hatching on longer parent lamellae, can be observed in the section. This morphology agrees very well with previous observations[12,13] and further confirms the DSC results: the crystals in the PP are of the $\alpha$-phase.

The image obtained at high magnification [Fig. 2(b)] also show that the amorphous regions are sandwiched between crystalline lamellae. The thickness of the amorphous layers is less than 10 nm. These observations are consistent with those of other semicrystalline polymers revealed by TEM and atomic force microscopy.[8,11–13,15,16] Even though the amount of all the amorphous materials in semicrystalline polymers is high, the thickness of the individual amorphous layers is very small.

### CB Distribution in the PP Matrix

The morphology of CB-filled PP composites and the CB distribution in the semicrystalline PP matrix were also investigated. Figure 3 shows the TEM micrographs of an ultrathin section of the sample filled with 10 wt % of N660 CB. Several important features are revealed.

First, as can be seen clearly from the TEM micrographs, the PP matrix of the composite also exhibits a morphology similar to that of the PP, a cross-hatched lamellar structure. This indicates that the PP matrix of the composite is the $\alpha$-phase, which is in total agreement with the DSC results. In particular, the thickness of the amorphous layers does not change much ($<$10 nm). The individual amorphous layers are very

**Table I Crystallinities, Melting Points, and Resistivities of PP and Different CBs-Filled PP Composites**

| Sample | PP | 10 wt % N660 | 10 wt % V-XC72 | 10 wt % EC300J |
|---|---|---|---|---|
| Crystallinity, wt % | 56.9 | 55.3 | 56.8 | 57.6 |
| Melting point, °C | 166.5 | 166.7 | 167.6 | 166.3 |
| Resistivity, ohm-cm | — | $9.8 \times 10^8$ | $5.0 \times 10^2$ | 9.1 |

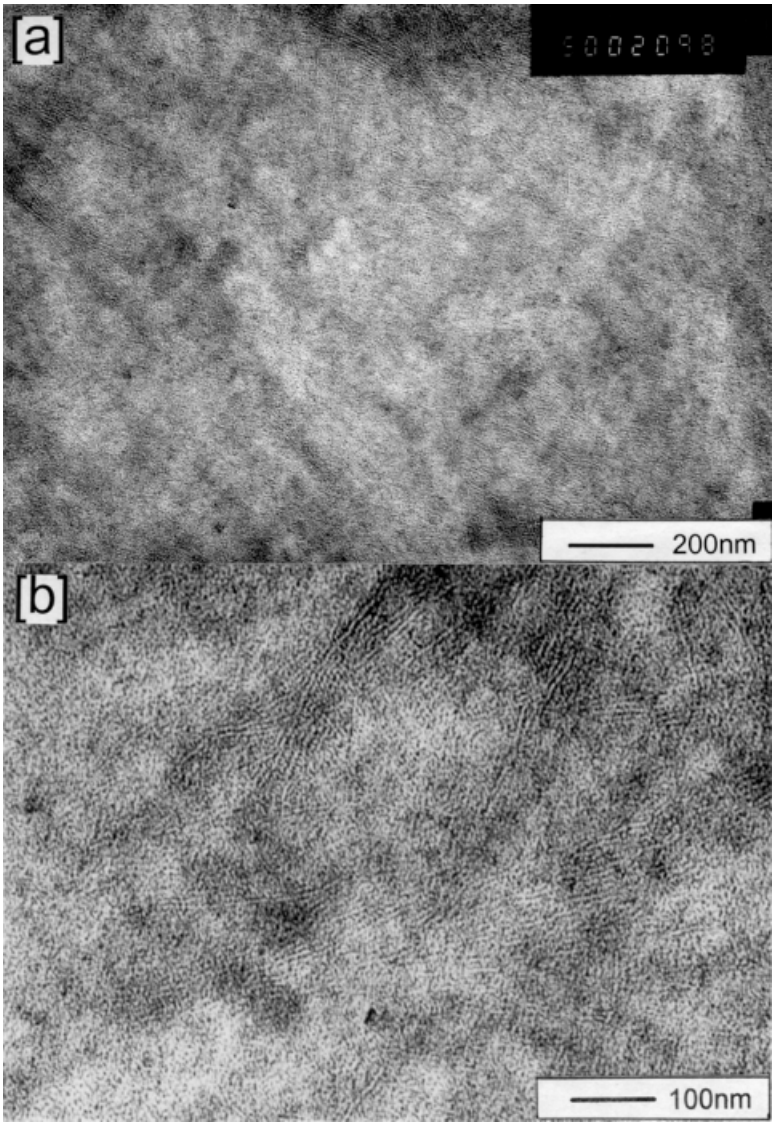


**Figure 2** TEM micrographs of an ultrathin section of PP stained with $RuO_4$ vapor.

thin, even though the crystallinity of the PP matrix is about 57 wt %.

Second, compared with the thickness of the lamellae or the amorphous layers, the CB particles or aggregates are very large, even in the finest conductive CB (EC-300J) investigated in the present work (see below at Fig. 5). The particle size of the CB is in the tens of nanometers range. Compared with the dimensions of the PP spherulites, the CB particles are extremely small. The diameter of the typical PP spherulites is about 100 $\mu$m, whereas the size of the N660 CB particles or aggregates is less than 100 nm. It has been speculated that the CB particles accumulate at or near the boundaries of the spherulites.[1–4] Our results clearly indicate that the CB particles and aggregates are not segregated at the spherulite boundaries but, rather, are distributed fairly uniformly within the spherulites. The TEM results suggest that the CB particles do not migrate long distances during crystallization. Perhaps the CB particles are not swept by advancing spherulitic fronts into the boundaries of spherulites during crystallization because they are too large compared with the lamellae.

Third, the TEM micrographs indicate that the CB particles are much darker than the PP matrix, for which there are two possible reasons. One is that the CB particles have a larger mass density than that of the PP matrix. The other is that the

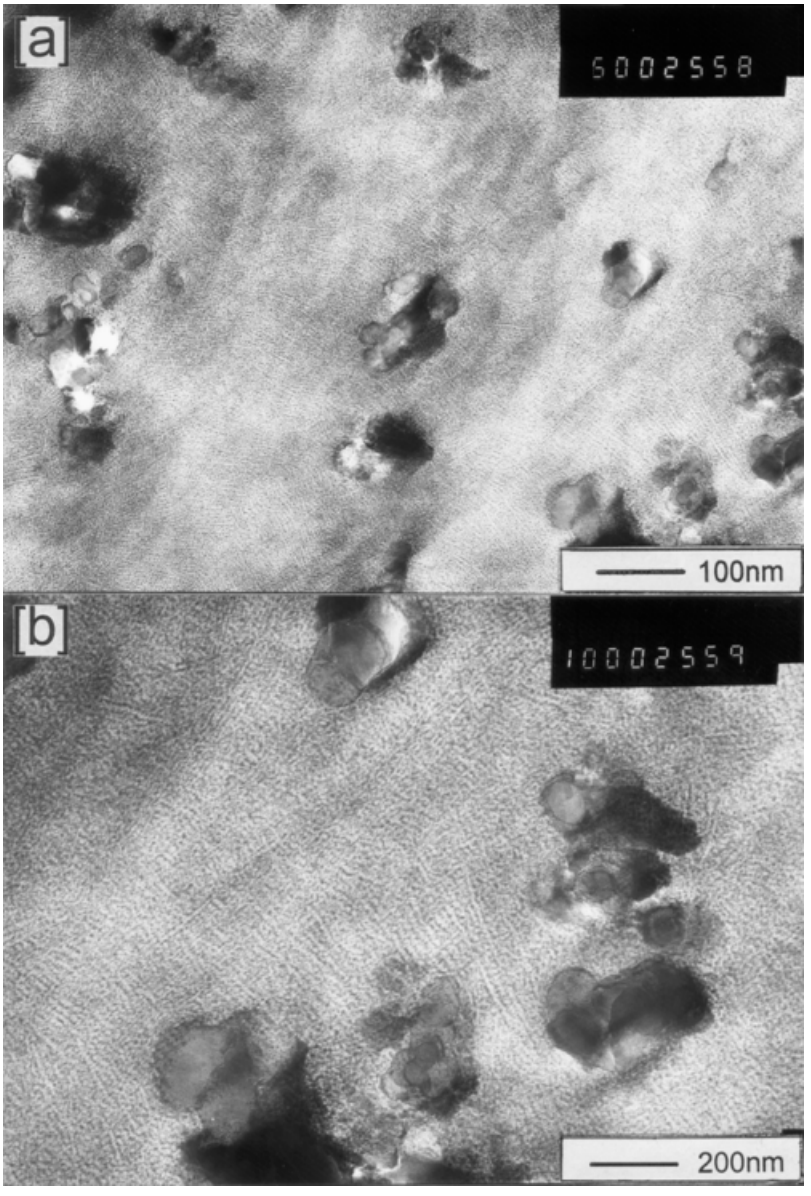


**Figure 3** TEM micrographs of an ultrathin section of 10 wt % N660-filled PP stained wtih $RuO_4$ vapor.

CB particle surface adsorbs some $RuO_4$ vapor. The combination of these two effects leads to a much stronger scattering ability of the CB particles, giving rise to much darker images of the CB particles in the PP matrix, as shown in the TEM micrographs.

Finally, the relationship between the CB particles or aggregates and the amorphous regions requires attention. After a careful examination of the TEM micrographs in Figure 3, it can be seen that a very thin continuous dark layer is present between the CB particles and PP matrix. The thickness of this thin layer, which is believed to consist of amorphous PP, is less than 10 nm or even smaller. Accordingly, the CB distribution in the semicrystalline PP matrix should follow the pattern of a thin layer of amorphous PP encapsulating the CB particles or aggregates. Karasek and Sumita[17] have shown that there is a layer of tightly bound rubber on the surface CB particles because of the polymer–filler interactions. A layer of bound polymer was also found in the high-density polyethylene/silica and PP/silica systems.[18] The thickness of this bound polymer was reported to be dependent on the filler concentration

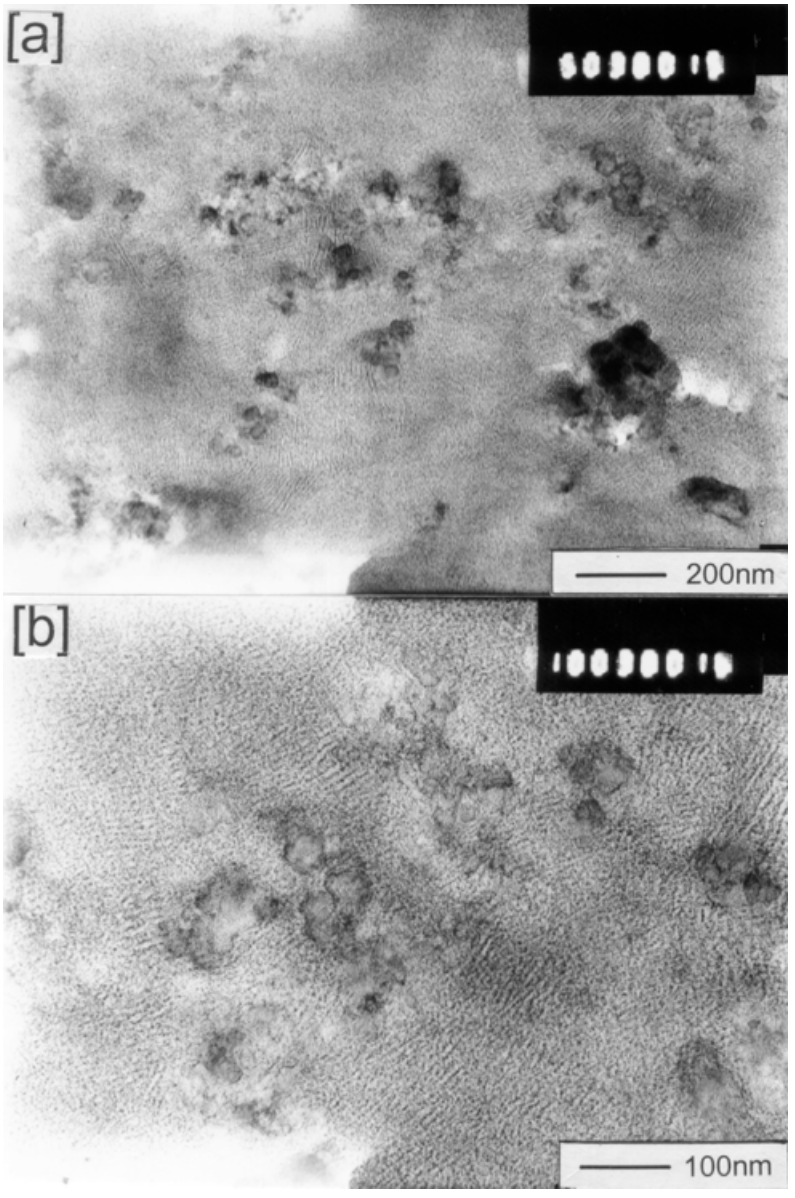


**Figure 4** TEM micrographs of an ultrathin section of 10 wt % V-XC72–filled PP stained with $RuO_4$ vapor.

and molecular weight of the polymer. For the PP/silica system (24 wt % silica), the thickness of the bound polymer was calculated to be about 4 nm.

To illustrate that our observations are general, two other CBs, V-XC72 and EC-300J, were used. The results for the samples filled with V-XC72 and EC-300J are shown in Figures 4 and 5, respectively. A comparison of all the TEM results seems to indicate that the conclusions about CB distribution in a semicrystalline PP matrix are general, even though the size of the CB particles varies. In addition, the TEM micrographs suggest that the size and distribution of the carbon black particles are important factors that determine the resistivity of the materials. The room-temperature resistivity of the composites filled with N660, V-XC72, and EC-300J was measured to be $9.8 \times 10^8$, $5.0 \times 10^2$, and 9.1 ohm-cm, respectively. These results show that the resistivity of the composites decreases as the particle size of the carbon black decreases because the interparticle distances decrease and the number of the conductive paths increases as the carbon black size decreases.

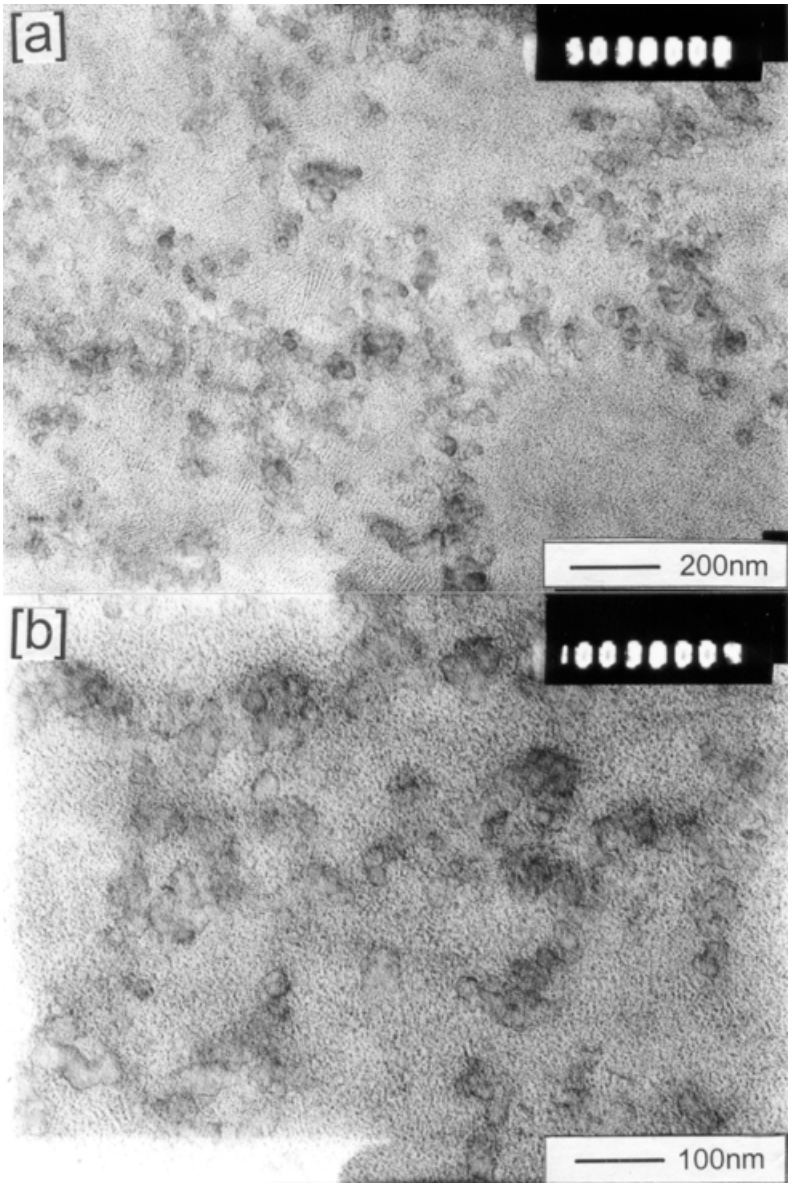


**Figure 5** TEM micrographs of an ultrathin section of 10 wt % Ketjenblack EC-300J–filled PP stained with $RuO_4$ vapor.

## CONCLUSIONS

This report provides experimental evidence about the CB distribution in a semicrystalline polymer matrix. We found that the amorphous PP regions are smaller than 10 nm, even though the sum of all amorphous materials is large, reaching 43 wt %. The CB particles or aggregates are distributed inside the spherulites and do not accumulate at the spherulitic boundaries. Between the CB particles and the PP matrix there is a thin layer of amorphous material encapsulating the CB particles.

This work was supported by the Industry and Technology Development Council (under Grant AF/155/99) and the Hong Kong Government Research Grant Council (under Grant HKUST 6123/97P).

## REFERENCES

1. Meyer, J. Polym Eng Sci 1973, 13, 462.
2. Meyer, J. Polym Eng Sci 1974, 14, 706.

3. Narkis, M.; Ram, A.; Stein, Z. J Appl Polym Sci 1980, 25, 1515.
4. Voet, A. Rubber Chem Technol 1981, 54, 42.
5. Al-Allak, M.; Bringkman, A. W.; Woods, J. J Mater Sci 1993, 28, 117.
6. Hanchett, V. E.; Geiss, R. H. IBM J Res Dev 1983, 27, 348.
7. Yu, G.; Zhang, M. Q.; Zeng, H. M.; Hou, Y. H.; Zhang, H. B. J Appl Polym Sci 1999, 73, 489.
8. Kanig, G.; Kolloid, Z. Z. Polymer 1973, 251, 782.
9. Kanig, G. J Cryst Growth 1980, 48, 303.
10. Grubb, D. T.; Keller, A. J Polym Sci Polym Phys Ed 1980, 18, 207.
11. Trent, S. J.; Scheinbeim, J. I.; Couchman, P. R. Macromolecules 1983, 16, 589.
12. Li, J. X.; Cheng, W. L. J Appl Polym Sci 1999, 72, 1529.
13. Li, J. X.; Ness, N. J.; Cheung, W. L. J Appl Polym Sci 1996, 59, 1733.
14. Li, J. X.; Cheung, W. L. Polymer 1999, 40, 1219.
15. Li, L.; Chan, C.-M.; Li, J. X.; Ng, K. M. Macromolecules 1999, 32, 8240.
16. Li, L.; Chan, C.-M.; Yeung, K. L.; Li, J. X.; Ng, K. M.; Lei, Y. Macromolecules 2001, 34, 316.
17. Karasek, L.; Sumita, M. Polymer 1996, 31, 281.
18. Akay, G. Polym Eng Sci 1990, 30, 1361.